STRUCTURE AND EVOLUTION OF AN OCEANIC MEGAMULLION ON THE MID-ATLANTIC RIDGE AT 27°N

By

Amy R. McKnight

B. A. , Geology
Colgate University, 1997

Submitted in partial fulfillment of the requirements of the degree of

Master of Science

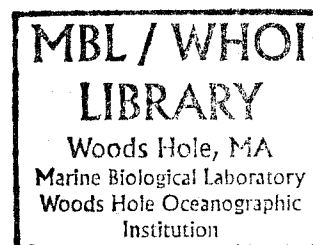at the

MASSACHUSETTS INSTITUTE OF TECHNOLOGY

and the

WOODS HOLE OCEANOGRAPHIC INSTITUTION

February 2001

Abstract

Megamullions in slow-spreading oceanic crust are characterized by smooth
"turtle-back" morphology and are interpreted to be rotated footwalls of long-lived
detachment faults. Megamullions have been analyzed in preliminary studies, but many
questions remain about structural and tectonic details of their formation, in particular how
the hanging wall develops in conjugate crust on the opposing side of the rift axis. This
study compares the structure of an off-axis megamullion complex and its conjugate
hanging wall crust on the Mid-Atlantic Ridge near 27°N. Two megamullion complexes,
an older (M1) and younger (M2), formed successively on the west side of the rift axis in
approximately the same location within one spreading segment. Megamullion M1 formed
while the spreading segment had only one inside corner on the west flank, and
megamullion M2 formed after the segment developed double inside corners west of the
axis and double outside corners east of the axis. The older megamullion formed between
~22.3 and ~20.4 Ma, and the younger megamullion formed between ~20.6 and ~18.3 Ma;
they are presently ~200-300 km off-axis.

Reconstruction poles of plate rotation were derived and plate reconstructions
were made for periods prior to initiation of the megamullion complex (anomaly 6Ar,
~22.6 Ma), after the termination of megamullion M1 and during the development of
megamullion M2 (anomaly 5E, ~19 9 Ma), and shortly following the termination of
megamullion M2 (anomaly 5C, ~17.6 Ma). These reconstructions were used to compare
morphological and geophysical features of both flanks at each stage of the megamullions'
development. Megamullion M1's breakaway occurred at ~22.3 Ma and slip along this
detachment fault continued and propagated northward at ~20.6 Ma to form the northern
portion of M2. The exhumed footwall of megamullion M1 has weak spreading-parallel
lineations interpreted as mullion structures on its surface, and it forms an elevated plateau
between the enclosing segment boundaries (non-transform discontinuities). There was an
expansion southward of the detachment fault forming megamullion M2 at ~20.1 Ma. It
either cut a new detachment fault through megamullion M1, stranding a piece of
megamullion M1 on the conjugate side (east flank), or it linked into the active detachment
fault that was forming megamullion M1 or propagated into its hanging wall. The
expanded detachment of megamullion M2 and the termination of megamullion M1
occurred during a time when the enclosing spreading segment roughly doubled in length
and formed two inside corners. Megamullion M2 developed prominent, high-amplitude
(~600 m) mullion structures that parallel the spreading direction for more than 20 km at
each inside corner. Its detachment fault was abandoned ~ 18.6 Ma in the south and ~18.3
Ma in the north.

The gravity of this area demonstrates a consistent pattern of higher gravity
corresponding to inside corners with thinner crust, apparently caused by fault exhumation
of deep lithosphere, and lower gravity values corresponding to outside corners, indicating
thicker crust, most likely a result of volcanic accretion. The gravity pattern of the area
also helps with interpreting evolution of the megamullion complex. The southern section
of megamullion M1 exhibits a series of inside-corner highs and elevated gravity values

while the northern section has lower gravity values until megamullion M2 began to form. This change coincides with the change of the northern segment edge from an outside corner to an inside corner. During the formation of megamullion M2, a gravity high developed over the center of the megamullion. After the termination of megamullion M2, the gravity values of both the northern and southern sections of the spreading segment decrease. This pattern suggests exhumation of higher-density lithosphere during formation of M1 and M2, and a return to more normal ridge-axis conditions following termination of the megamullion complex. The gravity of conjugate crust is consistently more negative, slightly decreasing in value during the formation of megamullion M2. This suggests that crust on the east flank is significantly thicker than that on the west flank, and that rift-axis magmatism may have slightly increased at the time that megamullion M2 formed.

We modeled gravity of an idealized structural cross-section of megamullion M2 to investigate possible structure and composition of the megamullion. Models with different detachment-fault angles and degrees of serpentinization of exhumed mantle that may be present in the megamullion were compared to Residual Mantle Bouguer Anomaly (RMBA) profiles. All models show gravity peaks slightly skewed towards the termination because higher-density rock is exposed closer to the termination than to the breakaway. Four models that varied the detachment fault angle show small variations that are unresolvable in the actual gravity data. Thus, the gravity profile of a megamullion is not diagnostic of its detachment fault angle from 30° to 60°/90°. Models that varied the degree of serpentinization of a lithospheric wedge beneath the megamullion show that slight variations in density give rise to large changes in the modeled gravity profiles. Comparison of model results against gravity profiles taken across megamullion M2 indicate that the magnitude of the gravity high associated with the megamullion is best explained by densities between 2800 kg/m^3 and 3000 kg/m^3 in the main body of the megamullion. This corresponds to peridotite serpentinized approximately 50%, or to gabbro (~2800 kg/m^3).

Table of Contents

1 Introduction

Detachment faults frequently develop on a sub-regional to regional scale in continental extensional environments; they are characterized by apparently normal, low-angle slip and displacement of tens of kilometers (Davis and Lister, 1988). It is common for the footwalls of detachment faults to expose middle to lower crustal metamorphic rocks (metamorphic core complexes). These rocks are believed to have undergone ductile deformation at depths greater than 10-15 km in the crust before undergoing brittle deformation during exhumation (Hodges et al., 1987). In comparison, the hanging wall may be thinned, but it consists of predominantly unaltered, unmetamorphosed rocks.

A similar kind of extension has been proposed to occur along mid-ocean ridges during periods of limited magma supply (Tucholke and Lin, 1994; Tucholke et al., 1996, 1997b; Cann et al., 1997). Bathymetric and sidescan-sonar images have revealed that areas with limited or intermittent magma supply sometimes exhibit domed massifs (megamullions) with corrugated surfaces (mullions). These domes span several kilometers to 20-30 km in diameter, are frequently up to 1. 5 km in relief, and have a surface interpreted to be the relict slip plane of a detachment fault. Many megamullions have been identified along the Mid-Atlantic Ridge, in the Australian-Antarctic Discordance, and on the Southwest Indian Ridge (Tucholke et al. 1996, 1998a; Cann et al., 1997; Casey et al., 1998; Dick et al., 1998; Fujioka et al., 1998). Additionally, there are incipient or poorly developed megamullions associated with areas of limited magma supply which are thought to represent proto-megamullions; i. e. , megamullions that were

unable to fully develop due to a lack of sustained slip along a single fault (Tucholke et al., 1998a).

Morphologically, the turtle-back footwalls of metamorphic core complexes are similar in relief and extent to oceanic megamullions (Wright et al., 1974; Armstrong, 1982; Stewart, 1983; Tucholke et al., 1998a). For example, continental metamorphic core complexes have similar wavelengths (several tens of kilometers) and amplitudes (a kilometer or greater) to oceanic megamullions (Wright et al., 1974; Stewart, 1983; Tucholke et al. 1998a). Therefore, megamullions are thought to represent an extreme case of asymmetric seafloor spreading, with domes containing lower crustal and upper mantle materials on the footwall side of a mid-ocean ridge axis and a volcanic hanging wall on the other side (Figure 1) (Tucholke et al., 1998a).

Individual megamullions have been studied previously, but this study is the first attempt to examine both a megamullion and its conjugate crust on the opposing side of the rift axis. Analysis of bathymetric, gravity, and sidescan-sonar data on both ridge flanks is essential to understanding rift-axis conditions immediately prior to the development of a megamullion, during its formation, and immediately following its termination. In this study, we first summarize what is known about megamullions. We then analyze the formation and evolution of a well developed megamullion and its conjugate through structural analysis based on multi-beam bathymetry and sidescan-sonar records, and geophysical analysis of Residual Mantle Bouguer Anomaly (RMBA) patterns. We also model the gravity signature of the megamullion based on a structural cross-section

predicted from the detachment fault model, and we compare the results to observed gravity data to constrain the structure and density of the megamullion.

2 Background

2.1 Segmentation along Mid-Ocean Ridges

Fundamental segmentation of the lithosphere is achieved by first-order (transform faults) and second-order (non-transform) ridge-axis discontinuities (Macdonald, 1986). Along slow-spreading ridges, discontinuities are associated with thinned or missing crust, and the crust in the corner between the active discontinuity and the spreading axis (inside corner) commonly exhibits irregular fault patterns with few volcanic features (Shaw, 1992; Shaw and Lin, 1993, 1996; Tucholke and Lin, 1994). Conversely, crust across the rift-axis along the inactive trace of the discontinuity (outside corner) has regular fault patterns, normal crustal thickness, and a regular distribution of volcanic features (Tucholke and Lin, 1994).

The accretion of magma along a slow-spreading ridge commonly appears to be focused at segment centers along the spreading axis (Whitehead et al., 1984: Crane, 1985; Lin et al., 1990). Compared to segment centers, segment ends at non-transform discontinuities along the Mid-Atlantic Ridge between 27°50'N and 30°40'N show large positive gravity anomalies equivalent to ~50% reduction in crustal thickness; in some cases, this accounts for a crustal-thickness variation of more than 3 km between segment

centers and segment ends (Lin et al., 1990). This observation argues that minor non-transform discontinuities are not merely surficial *en echelon* cracks resulting from external stresses, but rather they are fundamental geodynamic divisions, marking boundaries of magmatic segmentation beneath the ridge. Total variation in crustal thickness along a segment seems to be related to segment length; longer segments have consistently greater variations in Mantle Bouguer Anomaly (MBA) values (Lin et al., 1990).

Segment morphology is related to the gravity anomalies. Abyssal hills along inside corners, which form at the rift valley walls through growth of normal faults, are more widely spaced and have greater throw than those at segment centers (Shaw, 1992). These features frequently lie outside the approximate boundary of RMBA lows that are typically centered within a spreading segment (RMBA bullseyes), and they correlate with RMBA highs toward segment ends, suggesting that the amagmatic extension associated with the large faults contributes to crustal thinning at segment ends, or vice-versa (Shaw, 1992; Shaw and Lin, 1993).

Cross-rift structural asymmetry tends to be concentrated near first- and second-order discontinuities at segment ends. Inside and outside corners, both along the ridge axis and off-axis, exhibit differences in crustal composition, RMBA, and morphology. Relict inside corners, proceeding off-axis from the ridge along flow lines, consist of a series of inside-corner bathymetric highs (Dick et al., 1981; Karson and Dick, 1983; Karson, 1990). These highs commonly exhibit strongly positive RMBA of up to 25 mGal above values at segment centers (Tucholke and Lin, 1994) and expose plutonic rocks as well as mantle ultramafics (Dick et al., 1981; Tucholke and Lin, 1994). In contrast, outside corners are

8

typically covered by basalts and have lower relief and greater depths than inside corners (Severinghaus and Macdonald, 1988; Tucholke and Lin, 1994). Additionally, gravity values of outside corners are typically 10-20 mGal less than gravity values of inside corners (Tucholke and Lin, 1994).

2.2 Cyclicity of Melt Input

Analysis of gravity data suggests cyclicity of melt input along slow-spreading ridges. RMBA variations of 20 mGal or more along flow lines near segment centers have a periodicity of ~2-3 m. y. and imply crustal-thickness changes of at least 2 km (Tucholke and Lin, 1994; Pariso et al., 1995; Tucholke et al., 1997b, 1998a). It is likely that at this timescale, the variations are due to cycles of changing magmatism along the ridge axis. Gravity data also suggest that high-density material is not continuously emplaced at the inside corners; instead, peaks in gravity are sporadically distributed along the inside-corner trace outward from the ridge axis (Tucholke and Lin, 1994; Blackman et al , 1998). These gravity highs correlate with well developed inside-corner highs and megamullions, and they also are typically found where elevated RMBA (i.e. higher-density material) appears along-isochron over the remaining length of segments; this implies that they correlate with segment-wide reductions in magmatism and accompanying increases in tectonic extension.

Conditions during amagmatic and semi-magmatic periods may favor continued slip along existing faults rather than the creation of new faults. This would develop inside-

corner highs composed of gabbro and peridotite as continued slip along the faults would exhume deeper crust. In contrast, increased magmatism would weaken the axial lithosphere and promote formation of new faults there, thus making continued slip along the older fault unlikely; the inward jumping of new fractures would create small-throw faults and small abyssal hills of basaltic composition. This process may explain the variable and intermittent development of inside-corner highs (Tucholke et al., 1998a).

2.3 Megamullions

Megamullions form at inside corners and are interpreted to be rotated footwalls of long-lived detachment faults (Figure 1). Corresponding outside corners are interpreted to be the hanging walls in which volcanic upper crust accretes. This crust is stripped from the inside-corner footwall and is carried to the ridge flank opposite the megamullion (Tucholke et al., 1998a).

Morphologically, megamullions exhibit consistent characteristics. Proceeding from where the feature initiated, the structure of a megamullion begins with an isochron-parallel ridge that defines where the detachment fault nucleated. This "breakaway" zone is typically an abyssal hill (ridge) whose younger side is interpreted to be the remnant fault plane. Following the breakaway there is an area of depressed crust that is typically several hundred meters deeper than the breakaway ridge. This zone rarely exhibits mullion structures although it frequently has isochron-parallel ridges up to hundreds of meters in relief (Tucholke et al., 1998a). These ridges may be formed by high-angle normal

faults dissecting the detachment surface, or they may be klippen of the hanging wall stranded on the inside corner during slip on the detachment fault. Axis-ward from this depression, the dome of the megamullion rises as much as 1. 5 km. Its surface is corrugated by distinctive mullion structures with amplitudes ranging from below the lower limit of detection in conventional multi-beam bathymetry data (i.e., ~20 m) to 600 m (Tucholke et al., 1998a). These structures cap the surface of the exposure and are oriented parallel to flow lines and fault-slip direction. Long-distance continuity of mullions provide evidence that megamullions were formed by slip on single, long-lived faults. In one example next to the Atlantis Fracture Zone, 50–80% of the edifice exhibits mullion structures detectable with multi-beam bathymetry (Cann et al., 1997). The detachment surface off-axis may be dissected by high-angle normal faults that form in response to bending stresses during footwall rollover (Figure 1) (Manning and Bartley, 1994; Tucholke et al., 1998b). A megamullion is typically terminated in a valley-and-ridge structure parallel to the spreading ridge axis. It is thought that detachment faults are abandoned for one of two reasons: 1) a "ridge jump" forms a new fault nearer to the spreading axis, or 2) although rare, a rift propagates along axis to form a new fault (Tucholke et al., 1998a).

Dip angles of megamullion detachment faults within the lithosphere are uncertain. The fault surface on the older side of a megamullion dome often has cross-isochron dips between 0 to 10° away from the ridge axis. The fault dip at the termination averages 23° (plus or minus 8°) toward the ridge axis, which is likely a minimum value because of

block rotation during transport from the rift valley to the ridge flank (Tucholke et al.,

1998a). According to continental detachment fault models, the fault dip angle is expected

to be ~30° or less (Thatcher and Hill, 1995). Some observations over megamullions

appear to be consistent with this assertion; one study interpreted an intracrustal

reflection from Cretaceous inside-corner crust to be a convex-upward detachment fault

flattening updip from 30° to 20° within the basement and to less than 15° along the

exhumed surface (Ranero et al., 1997). It was also shown that the interpreted heave of

the fault was sufficient for normal extension to exhume lower crustal and upper mantle

rocks (Ranero et al. 1997; Ranero and Reston, 1999).

There is significant evidence to suggest that megamullions expose cross-sections of

the oceanic crust and have abnormally thin crust. Assuming 6-km-thick crust, a fault-dip

angle of 60° would expose mantle at the surface only 6. 9 km from the breakaway,

whereas the mantle would be exposed at the surface 8. 5 km and 12 km from the

breakaway for dip angles of 45° and 30° respectively. All rock dredges and submersible

sampling of the surfaces of currently identified megamullions have yielded serpentinized

peridotites and gabbros (Auzende et al., 1994; Cannat et al., 1995; Cann et al., 1997;

Casey et al., 1998; Tucholke et al., 1998a). In some cases, these rocks are exposed for

flow line distances of as much as 35 km (Dick et al., unpub). The exposures need not be

purely tectonic exhumation along faults in amagmatic rift environments. The presence of

intrusives and extrusives interspersed with ultramafic rocks, as suggested by sampled

gabbros (Tucholke and Lin, 1994; Dick et al., unpub.) and *in situ* volcanic cones on

detachment surfaces (Tucholke et al., 1998b), indicate that intrusive magmatism and perhaps even seafloor volcanism may occur while detachment faulting exhumes deep-crustal and upper-mantle rocks.

Megamullions often have well developed magnetic anomalies, yet they are believed to consist of plutonic intrusives and upper mantle. However, recent research indicates that these observations are not mutually exclusive. In their magnetic survey of 0-29 Ma off-axis crust on the Mid-Atlantic Ridge, Tivey and Tucholke (1998) found that crustal magnetization is rapidly attenuated off-axis, indicating that magnetization in extrusive lava becomes only a background value off-axis. From this observation and analysis of ridge-flank magnetic patterns, they concluded that much of the off-axis magnetic signature is likely to be contained in plutonic crust.

The RMBA patterns over megamullions indicate crustal thickness variations, and they assist in interpreting megamullion evolution. Megamullions typically have an RMBA 20 to 25 mGal higher than normal crust found at segment centers, which suggests a reduction in crustal thickness of more than 2 km. If there is significant serpentinization, 2 km is likely a minimum reduction (Minshull, 1996). Gravity highs over most megamullions are not located near the terminations where it is thought that the deepest crust and mantle should be exhumed (Tucholke et al., 1998a). Rather, they are centered between the breakaway and termination or are shifted toward the breakaway. An exception is a megamullion near the Atlantis Fracture Zone in which the RMBA high is strongly skewed toward the termination (Blackman et al., 1998).

Two explanations of this gravity shift toward the breakaway have been proposed. One postulates that as the detachment fault continues to slip, there is increased seawater penetration into the fault zone which causes greater serpentinization of the mantle and results in a reduction of footwall density toward the termination (Tucholke et al., 1998a). The other asserts that the gravity reduction towards the termination is caused by increased magmatism at the ridge axis, possibly related to cyclic magmatism (Tucholke et al., 1998a). The latter is consistent with submersible observations at Dante's Domes megamullion on the Mid-Atlantic Ridge at 26.6° N where small volcanic cones appear on the flat detachment surface near the termination (Tucholke et al., 1998b).

2.4 Study Area

A detailed geological and geophysical study was conducted in 1992 on the western flank of the Mid-Atlantic Ridge between 25°25'N and 27°10' N, from the ridge axis out to 26–29 Ma crust (Tucholke et al., 1997b). In 1996, the eastern conjugate flank was surveyed out to 26 Ma crust (Tucholke et al., unpub. 1996). Each cruise collected Hawaii MR1 sidescan sonar, Hydrosweep multibeam bathymetry, gravity, and magnetics (Figures 2 and 3). This comprehensive data set is ideal for a geophysical investigation of megamullions and their conjugate crust.

The study area is located between the Kane Fracture Zone and the Atlantis Fracture Zone in a region of the Mid-Atlantic Ridge that has no major transform offsets

along approximately 800 km of axis (Figure 2). Spreading centers instead are defined by a series of non-transform discontinuities (Sempere et al., 1993). As defined by bathymetry, sidescan-sonar records, and magnetic anomaly data, non-transform discontinuities delineate nine spreading segments in the study area (Figure 2). Some of these segments have been forming for more than 20 my.; all are subparallel to flow lines of relative plate motion and appear to have migrated independently of one another (Tucholke et al., 1997b; Tivey and Tucholke, 1998).

Within the study area there are at least six megamullions known (Tucholke et al, 1998a). A megamullion complex located on the western ridge flank between ~26°30' and 26°50' N and 46°45'W and 47°30' W, together with its east-flank conjugate, was chosen as the subject of the present study (Figures 4, 5). This complex is morphologically prominent and well developed, it has extensive survey coverage including the surrounding crust (Figures 2-5), and it exhibits well defined magnetic anomalies that allow accurate plate reconstruction of the crustal conjugates.

3 Methods

3.1 Geophysical Data

The study area has extensive multibeam bathymetry, sidescan sonar, gravity, and magnetics datasets. Ship tracks were oriented ~15-25° to plate flow lines in order to obtain significant sidescan-sonar backscatter from ridge-parallel structures while still obtaining potential-field data subparallel to flow lines (Tucholke et al., 1997b).

Hydrosweep multibeam bathymetry insonifies a seafloor swath equal to twice the water depth and it provided nearly 100% bathymetric coverage. The data were processed using "MB software" developed by Caress and Chayes (1996), with additional editing to reduce outer-beam edge effects. These data were then combined with GPS navigation data and gridded at 100 m to 500 m grid intervals.

HAWAII MR1 sidescan-sonar survey (north and south looking) was also performed on both ridge flanks. The sidescan-sonar system was towed ~100 m beneath the sea surface to acquire back-scatter imagery, and the data were processed and gridded assuming flat seafloor (Tucholke et al., 1997b).

The multibeam and sidescan-sonar datasets were used for structural interpretation of the megamullion and its conjugate (Figure 4a, 4b). Bathymetric maps (50 m contour interval) in conjunction with both north- and south-looking sidescan-sonar data were used to identify faults and to determine their sense and magnitude of offset. Both data sets were also used to identify and determine the extent of mullion structures. Megamullions are marked by an absence of ridge-parallel tectonic fabric and relatively little high-amplitude structure, unlike typical oceanic crust where sidescan-sonar records detect numerous ridge-parallel, inward-dipping faults. Flowline-parallel mullion structures are observable in both sidescan-sonar records and in shaded-relief bathymetric images where low-angle lighting accentuates the features (Figure 5).

The total magnetic field was measured in each survey using a towed proton-precession magnetometer. Both datasets were corrected for the regional field using the 1991 International Geomagnetic Reference Field (International Association of

Geomagnetism and Aeronomy, 1992) and merged with near-axis magnetics data from Purdy et al. (1990). The data were inverted for magnetization, but different processing parameters were used for data sets on the two ridge flanks. Both data sets had a similar range of long wavelengths filtered from their signal, but in processing the west-flank data a greater range of shorter wavelengths was filtered out than in the east-flank data (Tivey and Tucholke, 1998; Lin et al. unpub., 1997). This results in a more smoothed pattern of magnetic reversals in the west-flank data than in the east-flank data. This affects our ability to compare detailed magnetic patterns of the two flanks, but it does not affect our isochron interpretations. We used the magnetics data set only to identify isochrons to derive reconstruction poles and to determine sense of offset between spreading segments. Magnetic isochrons were identified on magnetization maps using the geomagnetic polarity timescale of Cande and Kent (1995). Both normal- and reverse-polarity isochrons were identified out to chron 8 on the eastern ridge flank and out to chron 13 on the western flank.

The gravity field of both ridge flanks was processed simultaneously to obtain free-air anomalies, and it was further reduced to obtain MBA values. This was done by subtracting from free-air values the attraction of the water/seafloor interface, plus the attraction of the crust/mantle interface assuming a uniform crustal thickness of 6 km; the assumed density of the water layer was 1030 kg/m^3, the crustal layer 2730 kg/m^3, and the mantle layer 3330 kg/m^3. RMBA values were then calculated by removing from the MBA values the effects of lithospheric cooling based on a thermal-age model (Phipps Morgan and Forsyth, 1988).

There is a marked difference between mean RMBA gravity values over the off-axis eastern and western ridge flanks in our study area (Figure 3). This contrast is regional and in some places is greater than 25 mGal, with east-flank values markedly less than west-flank values. This strong flank-to-flank asymmetry indicates that the origin of the difference cannot have been created on-axis. The more negative eastern values are likely due to the crust being at a higher temperature than the thermal-age model predicts, and/or thicker than normal. The most likely cause of such effects is hotspot influence, either from the Azores hotspot (~1900 km to the north-northeast) or the Great Meteor hotspot (~1300 km to the east-northeast).

Although the cause of the regionally reduced east-flank gravity is uncertain, we can determine the magnitude of the effect and remove it from our data to allow better comparisons of east- and west-flank gravity signatures. To do this, we determined the mean off-axis gravity value on each side (for all data points mapped in each reconstruction, as discussed later) and removed it from the data on that side, thus deriving values deviating from the mean. These data were plotted in the reconstructions discussed below. More detailed corrections were considered when we modeled gravity for reconstructed cross-sectional profiles. These are discussed in Section 5. 2. 3.

3.2 Derivation of Reconstruction Poles

To understand the evolution of the megamullion complex and its conjugate, we derived reconstruction poles for time periods prior to, during, and following megamullion

18

formation (chrons 6Ar, 5E, 5C) and rotated geological and geophysical data accordingly to simulate ridge-axis conditions at those times. The relative past positions of adjacent lithospheric plates can be derived by matching positions of marine magnetic anomalies and fracture zones on either side of the ridge axis (Klitgord and Schouten, 1986). If both plates remain completely rigid, the rotation that restores these features to the ridge axis for a given geologic time also restores the plates to their relative position at that time (Figure 6). The latitude and longitude of the reconstruction pole, and the rotation angle about the pole, uniquely describe the plate reconstruction. Uncertainty in these three quantities depends on the extent of the magnetic lineation picks (the length of the plate boundary represented by the data), the inherent uncertainties in the picks, and the distance from the center of the data to the derived pole. Even reconstructions for plate boundaries with closely spaced, high-quality data will have different rotation-parameter uncertainties that vary with the geometric relationship between the data points and the pole position (Stock and Molnar, 1983).

We derived reconstruction poles for chrons 6Ar, 5E, and 5C. Using these poles, we were able to rotate geological and geophysical data to simulate ridge-axis conditions prior to the initial breakaway of the megamullion complex (at anomaly 6Ar), during its formation (anomaly 5E), and immediately after its termination (anomaly 5C). We used a least-squares technique developed by Hellinger (1981) and modified by Chang (1988) to derive reconstruction poles. This method uses correlative isochron points on each plate as model segments and estimates each segment as a segment of a great circle. In reality, model segments are not great circles, but each segment is short and the error in this

approximation is negligible when compared to the errors in the data (Chang, 1988). Hellinger's method minimizes a least squares measure of fit as a function of the rotation parameters. The measure of fit represents a sum of squares of the weighted distances of fixed and a rotated data points for a given rotation (Hellinger, 1981). Chang (1988) modified this technique by using a spherical regression method to find concentrated error approximations.

The reconstructions made here for chrons 6Ar, 5E, and 5C are based on magnetic anomalies picked in spreading segments within our study area (Figures 2, 7, 8), within segments between the study area and the Atlantis Fracture Zone and the Kane Fracture Zone, and at both fracture zones so as to delineate the positions of these discontinuities. The points at which shiptracks cross the magnetic isochrons were picked as isochron data points (Figure 7); positions of these anomalies were assigned a 10-km error radius. Magnetic profiles published in the OMD atlas of the Mid-Atlantic Ridge between 22° and 38°N (Rabinowitz and Schouten, 1986) were also interpreted for selected spreading segments between Kane and Atlantis Fracture Zones; anomalies picked in these zones lengthened the plate boundary represented by the data and thus decreased the uncertainties in our reconstruction poles. Positions of these picks were assigned a 20-km error radius.

Additional points are needed to constrain rotations of anomaly picks to the correct conjugate segments. These are provided by fracture zone "pivot points," without which the Hellinger-Chang rotation may not necessarily rotate points to their conjugate

segments, but rather to locations elsewhere along their great circles. Fracture-zone data points were chosen by a two-step process. Magnetic anomalies 6Ar, 5E, and 5C in segments to the north and south of Atlantis and Kane fracture zones were identified from the published OMD profiles. The trend of each segment's anomaly was then projected onto detailed bathymetric maps of the fracture zones, and the intersections with the interpreted traces of the fracture zones were chosen to represent the fracture-zone positions in the model (Figure 8).

Once the reconstruction poles for chrons 6Ar, 5E, and 5C were finalized (Figure 9), we rotated west-flank gridded geophysical data to their conjugates for each time period (Figures 8,10-18). Rotations were performed using a function based on C. Tapscott's Fortran library, translated by P. R. Shaw, and modified for MATLAB by C. Denham (pers. comm., 2000). The function performs a point-by-point rotation by calculating the rotation matrix for a rotation of "angle" degrees about the "ijk"th Cartesian axis. The rotated data were then combined with unrotated, conjugate data along the corresponding isochrons.

4 Reconstruction Results

4.1 Reconstruction Poles

Reconstruction poles derived here are given in Table 1 together with poles from Klitgord and Schouten (1986) for other anomalies close in time, and these are plotted in Figure 9. The error ellipses of our derived poles represent the upper and lower surfaces

21

of the 95% confidence region. Inherent ranges of error result from uncertainties of the anomaly picks with respect to assigned errors, potential mis-assignment of picks to segments, and real "geologic noise" in magnetic-anomaly positions. The latter is particularly important at slow-spreading ridges, such as the present study, where variable crustal accretion and tectonism result in poorly developed and discontinuous magnetic anomalies (Vogt, 1986).

4.2 Reconstruction Discrepancies - Overlap and Underlap

Reconstructions based on derived poles for chrons 6Ar, 5E, and 5C regionally fit conjugate anomalies together well (Figures 8 a-c). However, at a finer scale (Figures 10,13,16) the fits are not perfect. Variations in fit between different segments are explained by the fact that different segments were in different tectonic and magmatic states at any given time; thus each segment may have recorded changes in the magnetic field differently. Consequently, no pole will perfectly align every segment with its conjugate at a given time. The derived poles represent a best fit along a much greater length of the ridge.

There are several mechanisms that could cause anomalous spacing of conjugate magnetic-anomaly pairs. Amagmatic (i.e., severe tectonic) extension may result in a partial recording of a magnetic signature, depending on the timing of a magmatic event relative to the tectonic extension. In this study, we identified isochrons at the peaks and troughs of the magnetization anomalies. Hence, if amagmatic extension truncated the

recording of a magnetic-polarity interval, then the interpreted anomaly peak (or trough) would correlate to a time older than the actual anomaly peak (or trough) and underlap would occur in reconstructions. If magmatism occurred only late in the magnetic-polarity interval, the opposite would happen, and overlap could appear in reconstructions.

Underlap may also result from the difference between the time at which a plutonic rock (e.g., gabbro) is emplaced at a ridge axis and the time at which it cools through its Curie temperature (its magnetic-signature age), compared to the time at which rapidly cooling basalt acquires its magnetic-signature age. Cande and Kent (1976) asserted that magnetic-polarity boundaries should mimic crustal isotherms. Therefore, because basalt cools quickly, its polarity boundaries are near-vertical and are locked in at the spreading axis, and its emplacement age and magnetic-signature age are the same. However, gabbro cools more slowly, its isotherms are sloped, and its magnetic-signature age is younger than its emplacement age, i.e., it is locked in *off*-axis. Therefore, isochrons of segments that contain unusually large amounts of gabbro relative to basalt would be farther apart in reconstructions than isochrons of segments which contain "normal" basaltic and gabbroic sections of oceanic crust (Figure 19). Unusually large amounts of gabbro could occur at segment ends in areas of reduced magmatism, where extrusive magmatism does not occur. Or, the relative amount of gabbro could be enhanced where it is exhumed by faulting at inside corners.

Reconstructions at chrons 6Ar and 5E exhibit underlap between the conjugate flanks of segments F/G (Figures 10-15). This indicates that these magnetic-anomaly pairs are spaced farther apart than normal, possibly because magmatism occurred only in the

23